Construction of a lung adenocarcinoma prognostic model based on KEAP1/NRF2/HO-1 mutation-mediated upregulated genes and bioinformatic analysis

WEI ZHU[1*], YE ZHANG[1*], LINGYUN YANG[2*], LU CHEN[1], CHAOBO CHEN[3,4], QIFENG SHI[1] and ZIPENG XU[3]

[1]Department of Pathology, Xishan People's Hospital of Wuxi City, Wuxi, Jiangsu 214105, P.R. China; [2]Department of Renal and Rheumatology, Affiliated Children's Hospital of Jiangnan University (Wuxi Children's Hospital), Wuxi, Jiangsu 214000, P.R. China; [3]Department of General Surgery, Xishan People's Hospital of Wuxi City, Wuxi, Jiangsu 214105, P.R. China; [4]Department of Hepatobiliary and Transplantation Surgery, The Affiliated Drum Tower Hospital of Nanjing University Medical School, Nanjing, Jiangsu 210000, P.R. China

Received August 27, 2024; Accepted January 6, 2025

DOI: 10.3892/ol.2025.14902

Abstract. Lung adenocarcinoma (LUAD) is a prevalent malignant tumor of the respiratory tract. The Kelch like ECH associated protein 1 (KEAP1)/nuclear factor erythroid 2-related factor 2 (NRF2)/heme oxygenase 1 (HO-1) axis serves a pivotal role in the occurrence and progression of LUAD. The present study aimed to identify specific genes regulated by mutations of the KEAP1/NRF2/HO-1 axis and to investigate their prognostic potential in LUAD, as well as their association with the tumor microenvironment. Immunohistochemistry was performed to assess the expression levels of KEAP1, NRF2 and HO-1 in LUAD tissues and to evaluate their association with clinical pathology. Sequencing data and clinical information were obtained from The Cancer Genome Atlas (TCGA)-LUAD and Gene Expression Omnibus (GSE68465) databases, whilst mutation information was sourced from the cBio Cancer Genomics Portal website. The R package 'limma' and Venn diagram were utilized to identify upregulated differentially expressed genes. Subsequently, a prognostic model was constructed using univariate Cox regression analysis and 101 machine learning methods. A nomogram of the prognostic model was generated to assess its efficacy in evaluating survival among patients with LUAD. The 'ImmuCellAI' and 'oncoPredict' R packages were used to compare and evaluate differences in immune cell infiltration and immunotherapy between high- and low-risk groups, as well as the sensitivity of LUAD to chemotherapy drugs. Compared with the group with negative expression, the results revealed that the group with positive expression of NRF2 and HO-1 exhibited advanced tumor, lymph node and clinical stages and a worse prognosis. A predictive model incorporating four genes (kynureninase, serpin family B member 5, insulin like 4 and γ-aminobutyric acid type A receptor subunit α3) was constructed based on KEAP1/NRF2/HO-1 mutation-mediated upregulated genes (KNHMUGs). Risk score was an independent prognostic factor for patients with LUAD (hazard ratio, 1.038; 95% confidence interval, 1.034-1.043; P<0.001). A nomogram was developed to predict the prognosis of patients with LUAD, which was validated as a reliable prognostic tool. The low-risk group exhibited higher immune cell infiltration, including $CD4^+$ T, $CD8^+$ T, natural killer (NK) and NKT cells, compared with the high-risk group. In addition, it demonstrated increased expression levels of immune checkpoint inhibitory genes such as cytotoxic T-lymphocyte associated protein 4, T cell immunoreceptor with Ig and ITIM domains, hepatitis A virus cellular receptor 2 and B and T lymphocyte associated protein. Moreover, it displayed enhanced sensitivity to immunotherapy. Drug sensitivity analysis revealed that the high-risk group exhibited increased sensitivity towards vinblastine, docetaxel and cisplatin, whereas the low-risk group showed increased sensitivity to BMS_754807, SB505124_1194 and JQ1_2172. In conclusion, a KNHMUGs-based gene signature was constructed in the present study, which holds promise as a biomarker for evaluating patient prognosis and guiding treatment by effectively assessing immunotherapy response and chemotherapy sensitivity in patients with LUAD.

Correspondence to: Dr Zipeng Xu, Department of General Surgery, Xishan People's Hospital of Wuxi City, 1128 Dacheng Road, Wuxi, Jiangsu 214105, P.R. China
E-mail: xuzipeng1989@126.com

Dr Qifeng Shi, Department of Pathology, Xishan People's Hospital of Wuxi City, 1128 Dacheng Road, Wuxi, Jiangsu 214105, P.R. China
E-mail: shiqifeng1969@sina.com

*Contributed equally

Key words: lung adenocarcinoma, Kelch like ECH associated protein 1/nuclear factor erythroid 2-related factor 2/heme oxygenase 1, mutation, prognostic model, tumor immune microenvironment, immunotherapy, drug prediction

Introduction

Lung cancer is the most common malignant tumor, ranking as the second most prevalent and lethal malignant tumor

globally (1). Lung cancer can be broadly classified into two main subtypes: i) Non-small cell lung cancer (NSCLC) and ii) small cell lung cancer, from both pathological and therapeutic perspectives. Lung adenocarcinoma (LUAD) is a pathological subtype of NSCLC, accounting for ~45% of all cases (2). Despite important advancements in molecular targeting, chemotherapy, radiation therapy and immunotherapy, the prognosis of LUAD remains unfavorable, with a 5-year overall survival rate of ~15% (3,4). Previous studies have demonstrated the pivotal role of genetic analysis in the diagnosis and treatment of lung cancer (5-7). For instance, the polymorphisms of the epidermal growth factor receptor are associated with side effects and outcome of tyrosine kinase inhibitor therapy administered to patients with NSCLC (5-7). Therefore, there is an urgent need for novel and effective screening methods based on genetic analysis to improve diagnostic accuracy and treatment efficiency, in order to improve the prognosis of patients with LUAD.

The Kelch like ECH associated protein 1 (KEAP1)/nuclear factor erythroid 2-related factor 2 (NRF2)/heme oxygenase 1 (HO-1) pathway serves a pivotal role in metabolic reprogramming, immune remodeling and treatment resistance in LUAD (8). In total, 20-30% of LUADs exhibit KEAP1 loss-of-function mutations, leading to aberrant activation of NRF2 and subsequently resulting in poor prognosis (9,10). KEAP1 mutations facilitate the progression of LUAD by augmenting glutamine metabolism and upregulating solute carrier family 33 member 1 expression (11,12). Furthermore, KEAP1-mutant tumors diminish dendritic cell and T cell responses, thus driving immunotherapy resistance in LUAD (13). NRF2, a transcription factor, serves a crucial role in the antioxidant pathway, promoting tumor cell growth, proliferation and drug resistance (14). NRF2 is the target of KEAP1 and abnormal activation of NRF2 is not only associated with KEAP1 mutations but also with gain-of-function mutations in NRF2 (15). Previous studies have found multiple gain-of-function mutation sites affecting NRF2 in LUAD (16). NRF2 mutations promote tumor cell immune escape by inhibiting stimulator of interferon response CGAMP interactor 1 activation (17). HO-1, which is regulated by NRF2, serves a crucial role as an antioxidant factor. When HO-1 expression is dysregulated, it can promote the proliferation of lung cancer cells and make them resistant to radiotherapy (18,19). However, several crucial and unresolved issues remain, encompassing the potential reclassification of LUAD based on KEAP1/NRF2/HO-1 mutations, the intricate interplay between KEAP1/NRF2/HO-1 mutations and the tumor microenvironment, as well as the strategic implementation of therapeutic interventions to effectively control tumor progression contingent upon KEAP1/NRF2/HO-1 mutations.

Therefore, the present study aimed to identify specific genes regulated by gene mutations of the KEAP1/NRF2/HO-1 axis and construct a prognostic model using upregulated genes. All patients were stratified into low- or high-risk groups based on the risk score, and the diagnostic efficacy was validated in both the training and test sets. Furthermore, the association between risk score and immune cell infiltration in the tumor microenvironment was explored and the individualized sensitivity to chemotherapy and immunotherapy were simultaneously predicted for each patient with LUAD.

Materials and methods

Validation of the expression of KEAP1, NRF2, HO-1 and Ki-67. Postoperative paraffin-embedded tissue blocks of patients with LUAD who underwent surgical procedures at Xishan People's Hospital of Wuxi City (Wuxi, China) between January 2020 and June 2023 were included in the present study. The inclusion criterion was a histologically confirmed diagnosis of LUAD, whilst the exclusion criteria were prior chemotherapy or radiation therapy. After selection, a total of 104 tissue wax blocks from patients with LUAD were included in the study. The patients consisted of 42 men and 62 women, with an mean age of 66.6 years (range, 32-92 years). The present study was approved by the Ethics Committee of Xishan People's Hospital (approval no. xs2023ky021).

Tissue sections (5 μm) were prepared and the expression of KEAP1, NRF2 and HO-1 was assessed using immunohistochemistry as previously described (19), using anti-KEAP1 (cat. no. ab226997; 1:100 dilution; Abcam) , anti-NRF2 (cat. no. ab313825; 1:100; Abcam), anti-HO-1 (cat. no. ab137749; 1:100; Abcam) and anti-Ki-67 (cat. no. ab230460; 1:100; Abcam) antibodies as the primary antibodies. The Elivision™ plus Polyer HRP (mouse/rabbit) IHC Kit (cat. no. KIT-9902; Maixin Biotech. Co., Ltd.) served as the secondary antibody reagent in this study.

Data acquisition. High-throughput sequence-fragments per kilobase of transcript per million mapped reads data and clinicopathological information of patients with LUAD were acquired from The Cancer Genome Atlas (TCGA)-LUAD database (https://portal.gdc.cancer.gov/). Gene expression and survival data associated with the GSE68465 (20) dataset were obtained from the Gene Expression Omnibus (GEO) database (http://www.ncbi.nlm.nih.gov/geo/). Gene mutation information for KEAP1, NRF2 and HO-1 was retrieved from the cBio Cancer Genomics Portal (cBioPortal) website (http://www.cbioportal.org/). The association between KEAP1, NRF2 and HO-1 expression levels and patient survival was analyzed using the Kaplan-Meier Plotter website (https://kmplot.com/analysis/index.php?p=service) (21). All patients diagnosed with lung adenocarcinoma across the 17 datasets were included in this study. All possible cut-off values between the lower and upper quartiles were computed and the best performing threshold was used as a cut-off.

Identification of mutation-associated differentially expressed genes. Based on the mutation information obtained from the cBioPortal website, 112 tumor samples were classified into the mutation group, 403 tumor samples into the wild-type group and 59 normal pulmonary tissues into the normal group. The 'limma' package in R (version 4.1.3; http://www.r-project.org) was utilized to identify differentially expressed genes ($\log_2$ fold-change >1; $P<0.05$) by comparing gene expression between the mutant group and both the wild-type and normal groups (22).

Construction of a prognostic model. Candidate genes in the TCGA-LUAD and GSE68465 datasets were initially screened using univariate Cox analysis. Subsequently, 101 combinations of algorithms were used to construct a prognostic model based on the leave-one-out cross-validation framework (23).

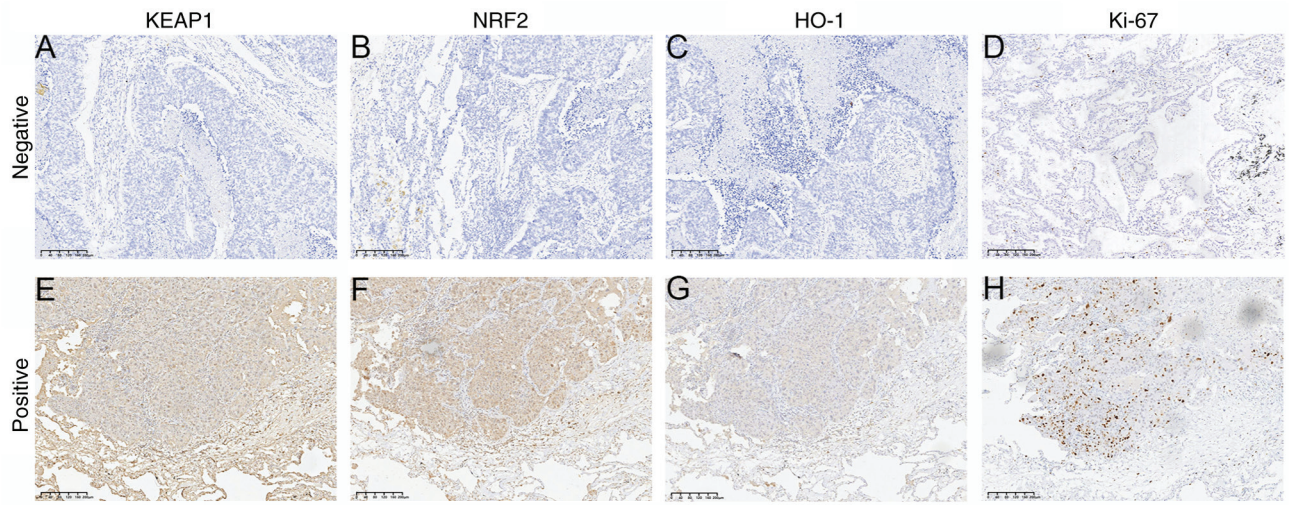

Figure 1. Immunohistochemical detection of KEAP1, NRF2, HO-1 and Ki-67 expression in lung adenocarcinoma tissues. Negative expression of (A) KEAP1, (B) NRF2, (C) HO-1 and (D) Ki-67. Positive expression of (E) KEAP1, (F) NRF2, (G) HO-1 and (H) Ki-67 (magnification, x100). KEAP1, Kelch like ECH associated protein 1; NRF2, nuclear factor erythroid 2-related factor 2; HO-1, heme oxygenase 1.

The TCGA-LUAD dataset was utilized as the training group, whilst the GSE68465 dataset served as the validation group. Furthermore, the consistency index (C-index) of each model was calculated in the validation group (23).

Survival analysis and nomogram construction based on clinical characteristics. Univariate and multivariate Cox regression analyses were used to identify independent prognostic factors in patients with LUAD. The 'rms' package in R (version 4.1.3) was utilized for constructing a nomogram based on risk score and two characteristic factors. Calibration curves were employed to evaluate the accuracy of these predictions. Additionally, decision curves generated using the 'rmda' package in R (version 4.1.3) were used to assess the predictive utility of the nomogram and to compare different prediction models.

Immune infiltration assessment and immunotherapy response prediction. The 'ESTIMATE' package in R (version 4.1.3) was used to evaluate the levels of immune cells and stromal cells in tumor tissues. The ImmuCellAI website (https://guolab.wchscu.cn/ImmuCellAI/#!/) was utilized for the analysis of immune cell types and levels within tumor tissues, facilitating a comparative assessment of immune cell levels between low- and high-risk groups (24). The effectiveness of immunotherapy in the aforementioned groups was evaluated through the prediction of individual response to immunotherapy among patients with LUAD.

Assessment of chemotherapy effectiveness. The 'oncoPredict' package in R (version 4.1.3) was used to predict chemotherapy drug sensitivity in patients with LUAD, aiming to compare the sensitivity to chemotherapy drugs between the high- and low-risk groups (25).

Expression of hub genes at the single-cell level. The Tumor Immune Single-cell Hub website (http://tisch1.comp-genomics.org/) was utilized to evaluate the expression of these hub genes in several cell types.

Statistical analysis. Statistical analyses were performed using R software (version 4.1.3). The Wilcoxon rank-sum test was used to determine the significance of differences between two groups. Frequency counts were used for statistical description of categorical (qualitative) data, and comparisons between groups were performed using either the χ^2 test or the Fisher's exact test. All P-values were two-tailed. $P<0.05$ was considered to indicate a statistically significant difference.

Results

Association between KEAP, NRF2 and HO-1 expression and clinicopathology. The expression of KEAP1, NRF2 and HO-1 was assessed using immunohistochemistry based on 104 cases of LUAD and their association with pathological characteristics was evaluated. The immunohistochemical analysis revealed that KEAP1 and HO-1 were predominantly expressed in the cytoplasm, whereas NRF2 and Ki-67 were primarily localized in the nucleus (Fig. 1). No significant association was demonstrated between the expression of KEAP1 and clinical features (Table I). Compared to the NRF2-negative group, the NRF2-positive group exhibited enhanced tumor aggressiveness, higher proportions of lymph node and distant metastases, more advanced TNM stage (26) and increased proliferative activity (Table I). Compared to the HO-1-negative group, the HO-1-positive group exhibited significantly higher grades in T stage, N stage, M stage and the overall TNM staging system. Additionally, the HO-1 positive group demonstrated a larger tumor diameter and a markedly increased expression level of Ki-67 (Table I).

Association between KEAP1, NRF2 and HO-1 expression and prognosis of patients with LUAD. The association between the expression of KEAP1, NRF2 and HO-1 and the prognosis of patients with LUAD was analyzed using the Kaplan-Meier Plotter website. The results indicated that, compared with low KEAP1 expression, high KEAP1 expression was not associated with overall survival (OS; Fig. 2A), but was significantly

Table I. Association between KEAP1/NRF2/HO-1 expression and clinicopathological features in lung adenocarcinoma.

A, KEAP1 expression

Clinicopathological feature	Positive (n=72)	Negative (n=32)	P-value
Age, years	66.04±11.58	67.78±11.15	0.47
Sex			0.80
Female	44	18	
Male	28	14	
T stage			0.06
T1-2	62	32	
T3-4	10	0	
N stage			0.50
N0	50	25	
N1-3	22	7	
M stage			0.09
M0	63	32	
M1	9	0	
TNM stage			0.12
I-II	54	29	
III-IV	18	3	
Tumor diameter, cm	2.01±1.44	2.10±1.03	0.72
Ki-67 expression ratio, %	41±15	39±13	0.37

B, NRF2 expression

Clinicopathological feature	Positive (n=58)	Negative (n=46)	P-value
Age, years	68.38±11.57	64.30±10.93	0.07
Sex			0.44
Female	37	25	
Male	21	21	
T stage			<0.01
T1-2	48	46	
T3-4	10	0	
N stage			<0.01
N0	34	41	
N1-3	24	5	
M stage			0.01
M0	49	46	
M1	9	0	
TNM stage			<0.001
I-II	39	44	
III-IV	19	2	
Tumor diameter, cm	2.52±1.50	1.43±0.68	<0.001
Ki-67 expression ratio, %	46±15	34±10	<0.001

C, HO-1 expression

Clinicopathological feature	Positive (n=63)	Negative (n=41)	P-value
Age, years	68.00±11.24	64.39±11.49	0.12
Sex			0.21
Female	34	28	
Male	29	13	

Table I. Continued.

C, HO-1 expression

Clinicopathological feature	Positive (n=63)	Negative (n=41)	P-value
T stage			0.02
T1-2	53	41	
T3-4	10	0	
N stage			<0.001
N0	36	39	
N1-3	27	2	
M stage			0.03
M0	54	41	
M1	9	0	
TNM stage			<0.001
I-II	42	41	
III-IV	21	0	
Tumor diameter, cm	2.43±1.50	1.42±0.64	<0.001
Ki-67 expression ratio, %	45±15	33±9	<0.001

Data are presented as n or the mean ± standard deviation. KEAP1, Kelch like ECH associated protein 1; NRF2, nuclear factor erythroid 2-related factor 2; HO-1, heme oxygenase 1; T, tumor; N, lymph node; M, metastasis.

associated with improved first progression survival (FPS; Fig. 2B). Conversely, high expression of NRF2 and HO-1 was significantly associated with worse OS and FPS, in comparison with low NRF2 and HO-1 expression (Fig. 2C-F). The association between KEAP1, NRF2 and HO-1 expression levels and disease-specific survival (DSS), disease-free interval and progression-free interval (PFI) were further assessed based on data from the TCGA-LUAD dataset. The results revealed that only the expression of HO-1 was significantly associated with poor DSS and PFI (Fig. S1).

Identification of KEAP1/NRF2/HO-1 mutation-mediated upregulated genes (KNHMUGs). From the cBioPortal database, KEAP1, NRF2 and HO-1 mutations in LUAD from TCGA pan-cancer atlas, which included 566 patients, were analyzed. Genetic alterations, such as in-frame, missense and truncation mutations of KEAP1 (19%), NRF2 (4%) and HO-1 (1.8%), were identified in patients with LUAD (Fig. 3). Based on the status of KEAP1/NRF2/HO-1 mutations, patients were classified into two groups: i) Mutant and ii) wild-type. Subsequently, the differential genes between the mutant, wild-type and normal groups were compared. A total of 2,346 upregulated genes specific to the mutant group were identified compared with the normal group (Fig. 4A), with 253 upregulated genes in the mutant group compared with the wild-type group (Fig. 4B). Furthermore, 172 common differentially upregulated genes in the mutant group were identified using a Venn diagram (Fig. 4C).

Prognostic model based on KNHMUGs. Univariate Cox regression analysis was then performed on 172 candidate genes in the TCGA and GSE68465 datasets. The TCGA dataset identified a total of 53 genes associated with prognosis, whereas the GSE68465 dataset revealed 29 genes that were prognostically relevant. Ultimately, an overlap of 21 genes with prognostic significance was observed in both datasets (Fig. 4D). Subsequently, these 21 genes were subjected to analysis using a combination of machine algorithms (101 combinations) with TCGA as the training set and GSE68465 as the validation set. By evaluating the C-index of both sets and considering the number of genes in optimal combinations, StepCox (backward) + random survival forest (RSF) algorithms emerged as the most effective prediction model (Fig. 5A), comprising four characterized genes, kynureninase (KYNU), serpin family B member 5 (SERPINB5), insulin like 4 (INSL4) and γ-aminobutyric acid type A receptor subunit α3 (GABRA3). Based on the median risk score, patients were stratified into high- and low-risk groups. Notably, OS was significantly lower for patients classified as high-risk compared with that for patients categorized as low-risk in both the TCGA [hazard ratio (HR), 12.21; 95% confidence interval (CI), 8.00-18.64; P<0.001] and GSE68465 (HR, 1.36; 95% CI, 1.05-1.75; P=0.012) datasets (Fig. 5B and D). It was also observed that the survival rate of patients significantly decreased as the risk score increased. Notably, the KYNU, SERPINB5, INSL4 and GABRA3 genes were identified as risk factors with an increasing trend in expression as the risk score rose (Fig. 5C and F).

Association between risk score and clinicopathological features. The association between risk score and clinicopathological characteristics was assessed. Patients with advanced-stage tumors [tumor stage (T) 3-4; lymph node stage (N)1-3; and stage III-IV] demonstrated a significantly higher risk score compared with those with early-stage tumors (T1-2; N0; and stage I-II), suggesting that this could be one of the

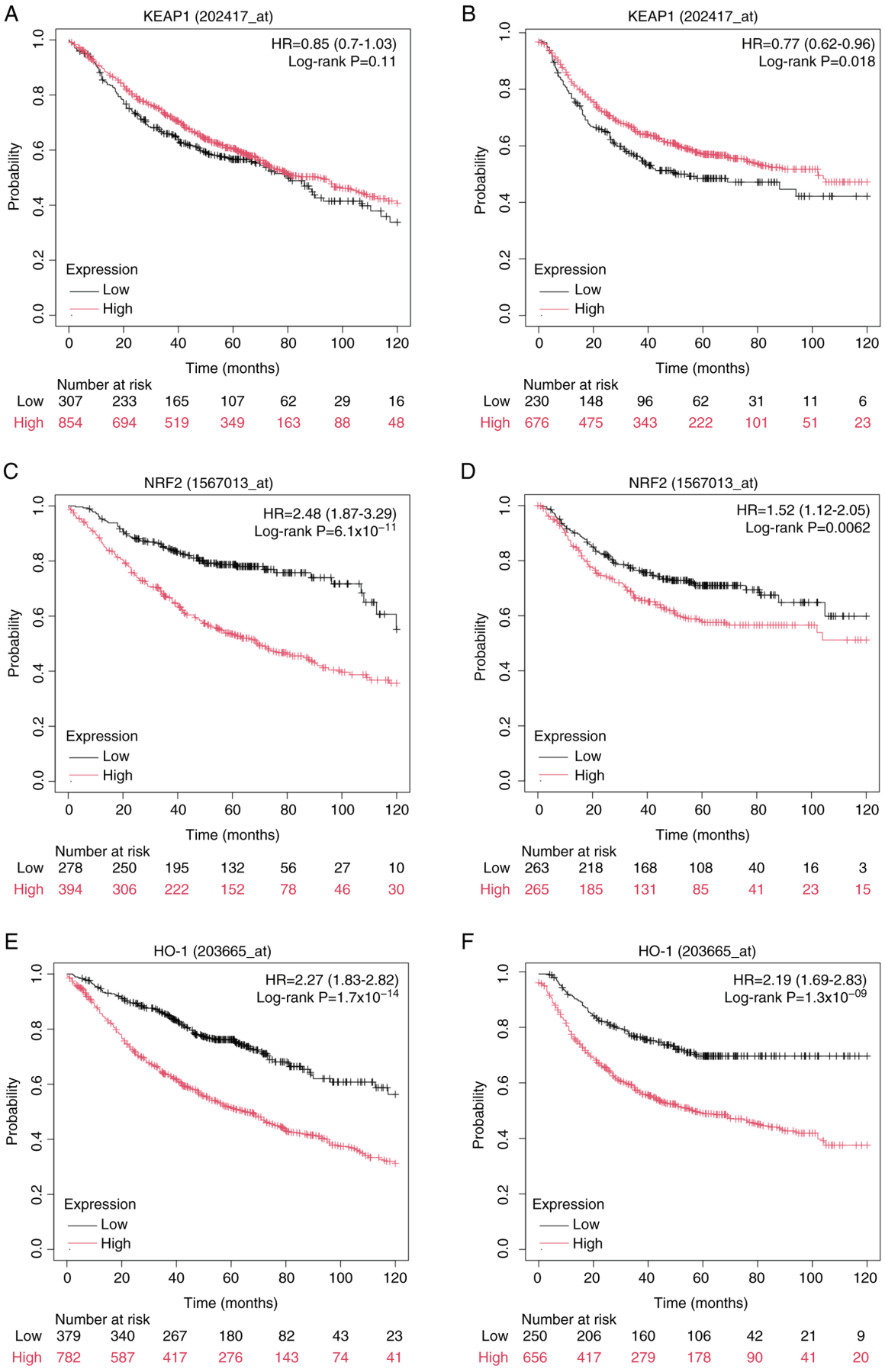

Figure 2. Association between KEAP1, NRF2 and HO-1 expression and prognosis of patients with lung adenocarcinoma. Kaplan-Meier survival curves of (A) overall survival and (B) first progression survival for KEAP1; (C) overall survival and (D) first progression survival for NRF2; and (E) overall survival and (F) first progression survival for HO-1 expression. KEAP1, Kelch like ECH associated protein 1; NRF2, nuclear factor erythroid 2-related factor 2; HO-1, heme oxygenase 1; HR, hazard ratio.

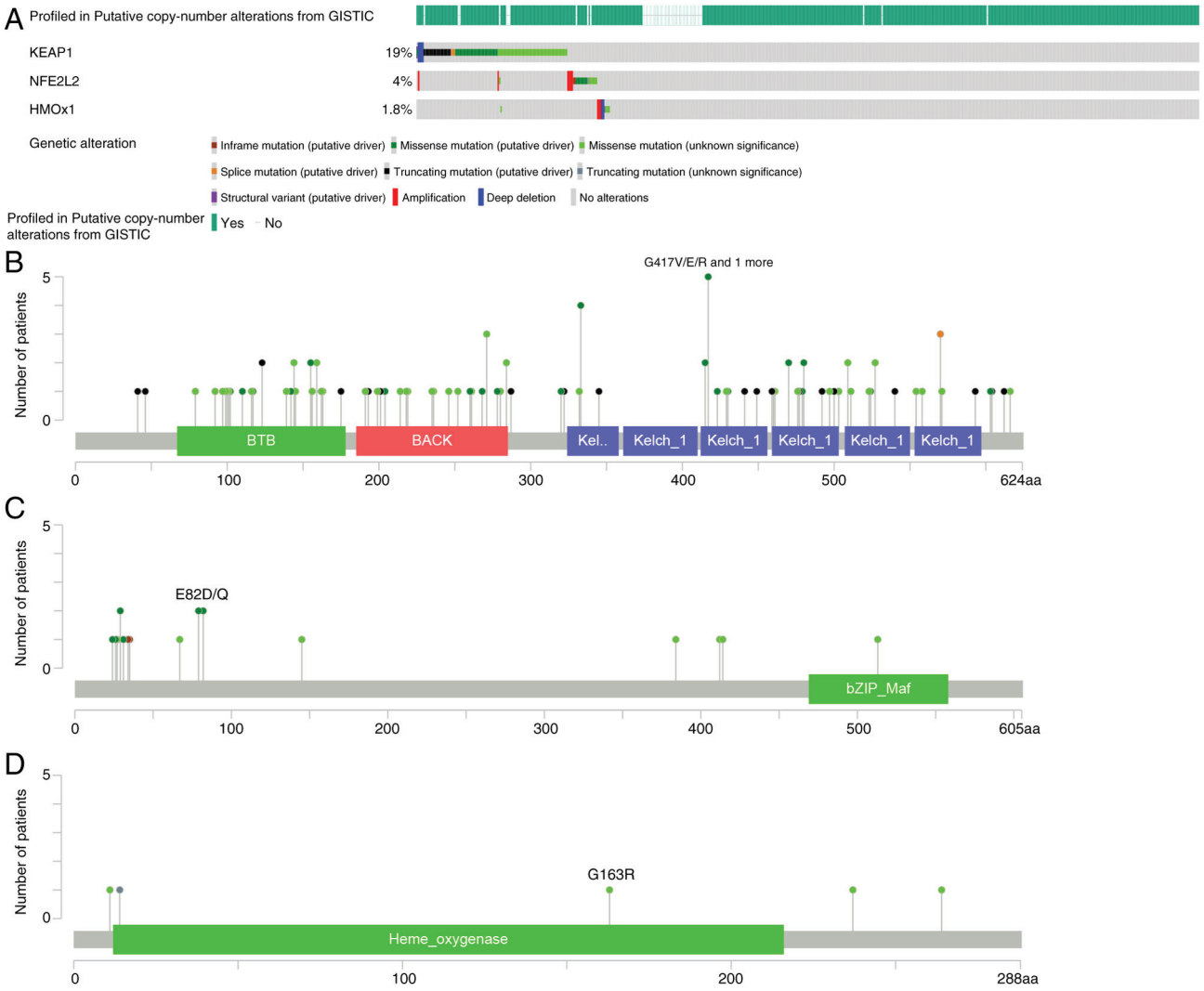

Figure 3. Overview of genetic changes in KEAP1, NRF2 and HO-1 mutations in patients with lung adenocarcinoma in The Cancer Genome Atlas database. (A) Types and frequencies of KEAP1, NRF2 and HO-1 genetic alterations. Lollipop charts of the genetic localization of (B) KEAP1, (C) NRF2 and (D) HO-1 mutations. KEAP1, Kelch like ECH associated protein 1; NRF2, nuclear factor erythroid 2-related factor 2; HO-1/HMOX1, heme oxygenase 1; GISTIC, genomic identification of significant targets in cancer.

factors contributing to the unfavorable prognosis observed in the high-risk group (Fig. 6A-C).

Construction of the nomogram. Univariate and multivariate Cox regression analyses were performed to assess the clinical characteristics and risk score of 490 patients (Fig. 6D and E). The results of the multivariate regression analysis revealed that risk score, N stage and metastasis (M) stage independently served as prognostic factors for patients with LUAD. Consequently, a nomogram was constructed based on these three independent risk factors (Fig. 6G) and calibration curves demonstrated a notable agreement between the predicted and actual values of the prediction model at 1, 2 and 3 years (Fig. 6F).

Association of risk score with immune infiltration and immunotherapy. The ESTIMATE results revealed that the low-risk group had significantly increased stromal and immune scores compared with the high-risk group, indicating a higher level of immune cell infiltration within this group (Fig. 7A). Subsequently, further analysis on immune cell infiltration in tumor tissues was performed. It was revealed that the low-risk group exhibited significantly enhanced infiltration of $CD4^+$ naive, $CD8^+$ naive, $CD4^+$ T, $CD8^+$ T, natural killer (NK), NKT cells and other immune cells compared with the high-risk group (Fig. 7C). Additionally, the expression levels of immune checkpoint-related genes were assessed. Notably, the low-risk group demonstrated a significantly increased expression of immune checkpoint-stimulated genes such as CD27, CD80 and C-X3-C motif chemokine ligand 1, as well as immune checkpoint-inhibited genes such as cytotoxic T-lymphocyte associated protein 4 (CTLA4) and hepatitis A virus cellular receptor 2 (HAVCR2), compared with the high-risk group (Fig. 7D and E). Furthermore, the efficacy of immunotherapy in different subgroups was predicted, and it was revealed that immune-checkpoint blockade therapy response prediction indicated a higher rate of response in the low-risk group compared with that in the high-risk group (Fig. 7B).

Association of risk score with drug therapy. The 'oncoPredict' R package was used to compare the differences in chemotherapy

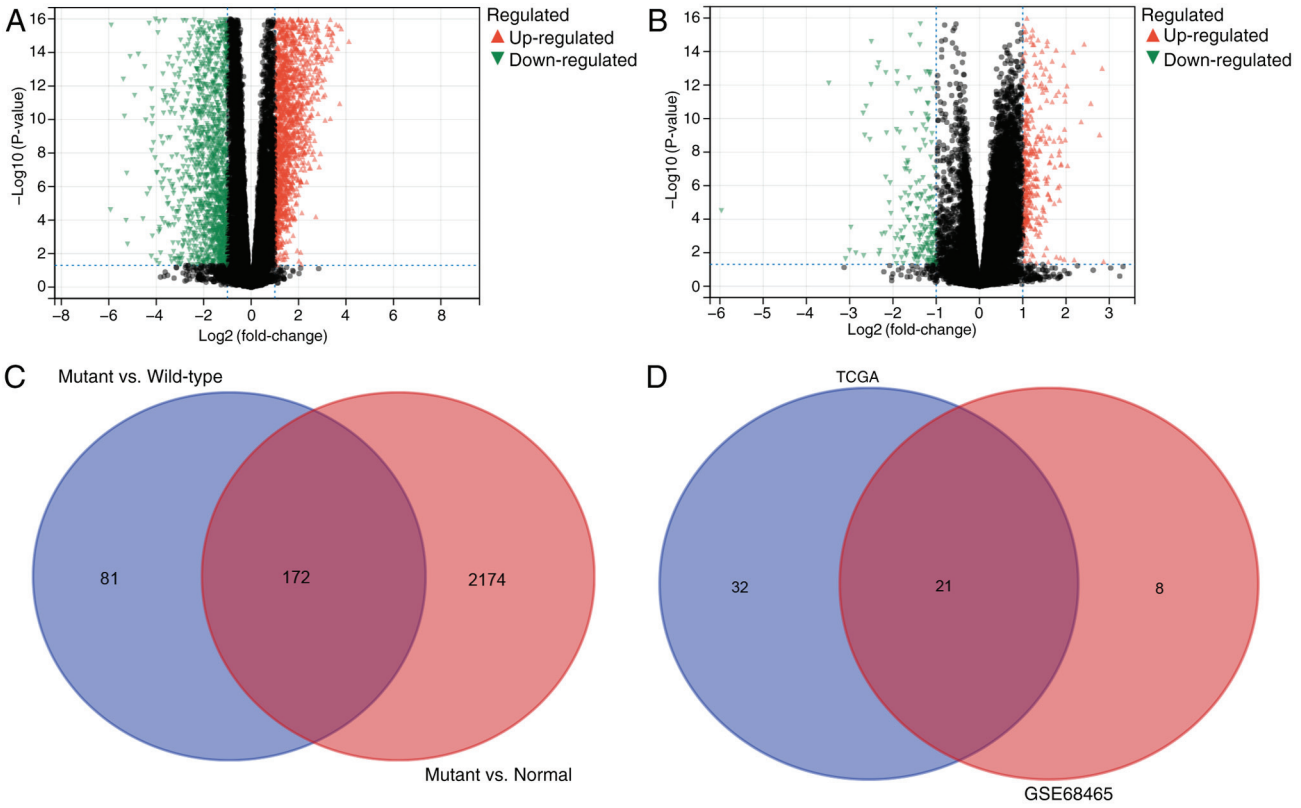

Figure 4. Prognostic-related genes upregulated by mutations in lung adenocarcinoma. Volcano plot of differentially expressed genes in the (A) t mutant vs. normal groups and (B) mutant vs. wild-type groups. (C) Common differential genes of mutant group vs. normal group and mutant group vs. wild-type group. (D) Common prognosis-related genes between The Cancer Genome Atlas and GSE68465 datasets.

sensitivity between the high- and low-risk groups. The results demonstrated that the high-risk group had a significantly increased sensitivity to vincristine, docetaxel and cisplatin, whilst the low-risk group exhibited a significantly increased sensitivity to BMS_754807 (insulin receptor inhibitor), SB505124_1194 (TGF-β receptor inhibitor) and JQ1_2172 [bromodomain and extraterminal (BET) inhibitor] (Fig. 8).

Expression of hub genes in different risk groups and their localization in LUAD. To analyze the expression of hub genes in different risk groups, the mRNA expression levels of hub genes were assessed. The findings revealed that KYNU, SERPINB5, INSL4 and GABRA3 were significantly upregulated in the high-risk group compared with that of the low-risk group ($P<0.05$; Fig. 9A). Additionally, the Tumor Immune Single-cell Hub website was utilized to evaluate the expression of these hub genes in several cell types. Annotation analysis of the GSE148071 single-cell dataset demonstrated that tumor tissue consists of diverse cells, including malignant cells, epithelial cells and fibroblasts. Notably, KYNU, SERPINB5, INSL4 and GABRA3 exhibited a predominant expression in malignant cells (Fig. 9B). These results suggest that these hub genes primarily contribute to LUAD progression by modulating biological functions, specifically within malignant cells.

Discussion

A total of 20-30% LUAD tumors carry mutations in KEAP1 and NRF2. Both loss-of-function mutations in KEAP1 and gain-of-function mutations in NFE2-like BZIP transcription factor 2 can activate the KEAP1/NRF2 pathway in LUAD (15). Previous studies have demonstrated that the KEAP1/NRF2/HO-1 axis inhibits cisplatin-induced ferroptosis by upregulating the iron death-related genes solute carrier family 7 member 11 and NAD(P)H quinone dehydrogenase 1 (27,28). Furthermore, the NRF2/HO-1 axis could attenuate resistance to programmed cell death 1 immunotherapy by inhibiting the transformation of M2 into M1 macrophages (29). Notably, KEAP1/NRF2 mutations are considered a pivotal driver of immune-suppressive tumor microenvironment metabolic reprogramming in LUAD, including potent induction of T-regulatory cells and diminishing the number of dendritic cells and tissue-resident memory CD8+ T cells, thereby compromising the efficacy of immunotherapy (13,30,31). However, combination therapy involving glutaminase inhibition and immune checkpoint blockade is reported to hold promise for reversing the immune suppression mediated by KEAP1/NRF2 mutations (13,30). Mutations in the KEAP1/NRF2/HO-1 genes serve a crucial role in the development of LUAD. However, there is a lack of established clinical models to assess the prognosis, tumor microenvironment and response to chemotherapy and immunotherapy in patients with LUAD based on genes regulated by KEAP1/NRF2/HO-1 mutations.

The prognostic model in the present study consisted of four genes: KYNU, SERPINB5, INSL4 and GABRA3. KYNU acts as a key enzyme in tryptophan metabolism, and its metabolite 3-hydroxyanthranilic acid is notably associated with poor

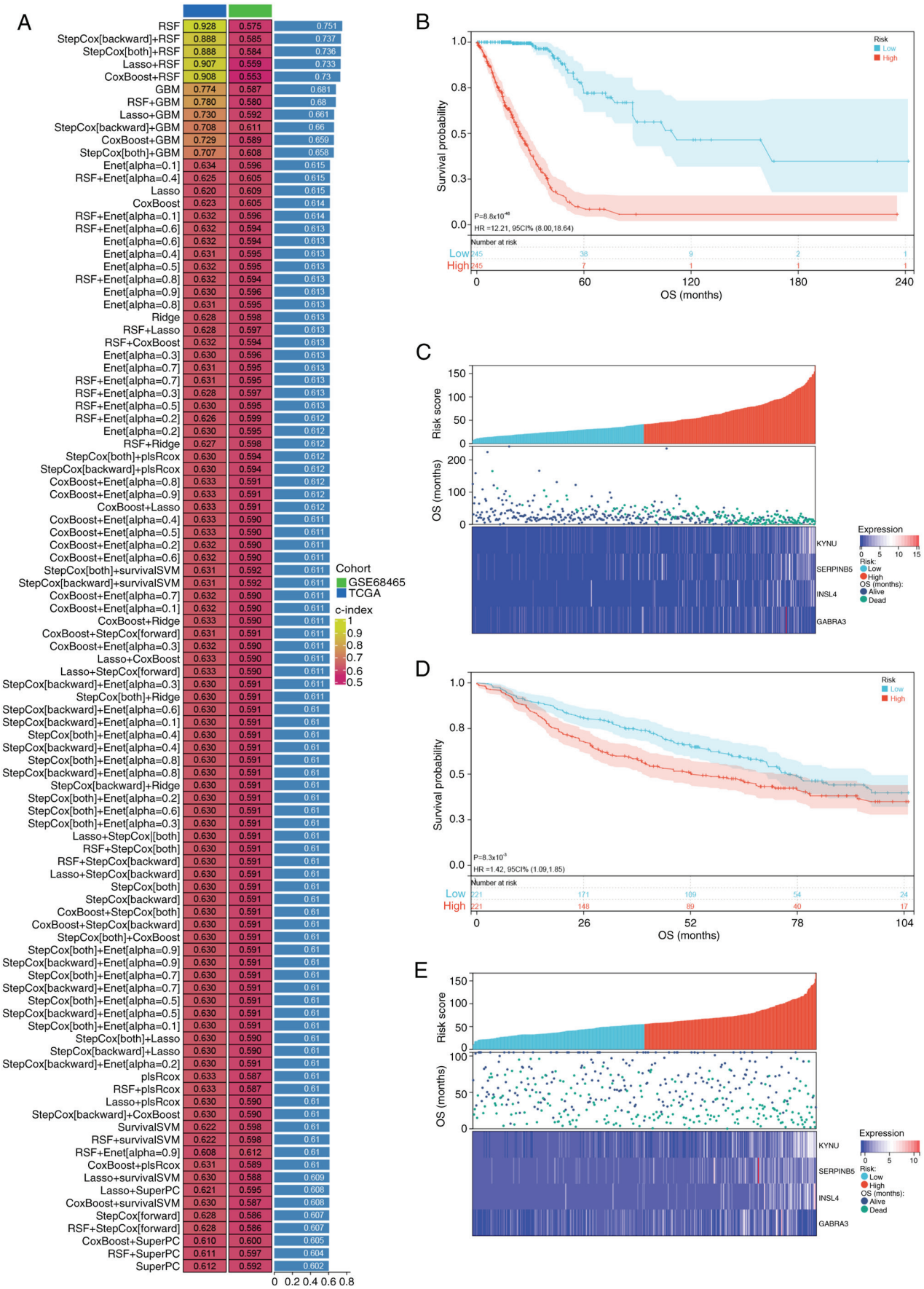

Figure 5. Construction of a prognostic signature based on KEAP1, NRF2 and HO-1 mutation-mediated upregulated genes. (A) A total of 101 types of prediction models were constructed via a leave-one-out cross-validation framework and the C-index of each model was further calculated. Kaplan-Meier survival curves of OS for high- and low-risk groups of patients in the (B) TCGA and (D) GSE68465 databases. Risk curves of the prognostic risk model in the (C) TCGA and (E) GSE68465 databases. TCGA, The Cancer Genome Atlas; OS, overall survival; KYNU, kynureninase; SERPINB5, serpin family B member 5; INSL4, insulin like 4; GABRA3, γ-aminobutyric acid type A receptor subunit α3; HR, hazard ratio; CI, confidence interval.

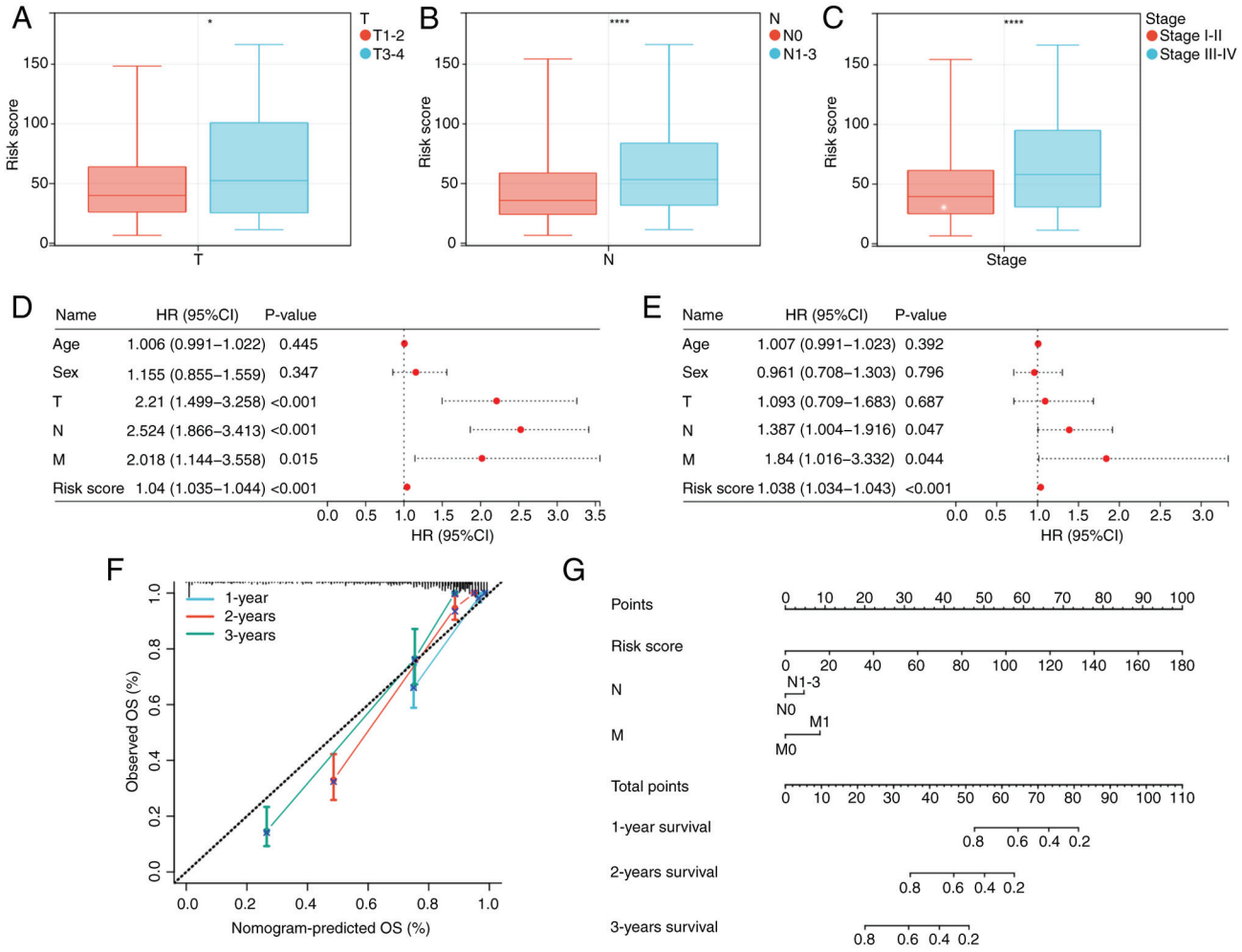

Figure 6. Clinical pathological features and prognosis analysis. Discrepancies in risk score in (A) T, (B) N and (C) TNM stages. Independent prognostic predictors obtained by (D) univariate and (E) multivariate Cox analyses. (G) Nomogram of risk score, N stage and M stage. (F) Calibration curve of the nomogram. *P<0.05, ****P<0.0001. T, tumor; N, lymph node; TNM, tumor-lymph node-metastasis; HR, hazard ratio; CI, confidence interval; OS, overall survival.

prognosis in patients with NSCLC (32,33). Further research reported that NRF2 upregulated KYNU, which was positively associated with an inhibitory tumor microenvironment (34). SERPINB2 belongs to the family of protease inhibitors, which is associated with tumorigenesis and regulation of several vital biological processes (35,36). The expression of SERPINB5 has been reported to be upregulated in LUAD, and its high expression levels were notably associated with poor OS. Furthermore, overexpression of SERPINB5 promoted cell proliferation, migration and invasion and epithelial-mesenchymal transition (EMT) in LUAD cells (37). INSL4 is a member of the insulin superfamily, which includes genes for insulin, insulin-like growth factors and relaxin. In LUAD, high levels of INSL4 expression have been reported to be associated with poor prognosis (38). Increased expression of INSL4 can promote tumor cell proliferation and invasion (38,39). GABRA3 acts as a key chloride ion transporter and also functions as a subunit of γ-aminobutyric acid A receptors (40). In LUAD, increased expression of GABRA3 has been closely associated with poor prognosis. By upregulating the expression of MMP-2 and MMP-9 via activation of the JNK/activator protein-1 signaling pathway, GABRA3 facilitates lymphatic metastasis in LUAD (41). Therefore, the aforementioned four genes are associated with the pathogenesis and progression of LUAD and may be considered potential therapeutic targets. Currently, there are studies investigating the regulatory association between KEAP1, NRF2 and HO-1 and KYNU (34). Subsequent research should further explore the interaction between KEAP1, NRF2 and HO-1, and SERPINB5, along with INSL4 and GABRA3.

The tumor microenvironment consists of diverse immune cells, stromal cells, extracellular matrix and several cytokines (42). These different components not only impact patient prognosis but also have a close association with immunotherapy (43). The present study revealed that the low-risk group exhibited a higher percentage of infiltration of $CD4^+$ T, $CD8^+$ T, NK and NKT cells compared with the high-risk group. Previous research has demonstrated that an increased presence of $CD4^+$ T and $CD8^+$ T cells is associated with improved prognosis and enhanced immunotherapeutic efficacy (44). NK cells are a subset of innate immune cells capable of rapidly recognizing and eliminating tumor cells whilst also promoting adaptive T-cell immune responses to suppress tumor aggressiveness (45). NKT cells represent a class of lymphocytes expressing both NK and T cell surface markers. They serve as a link between intrinsic and adaptive immunity and serve

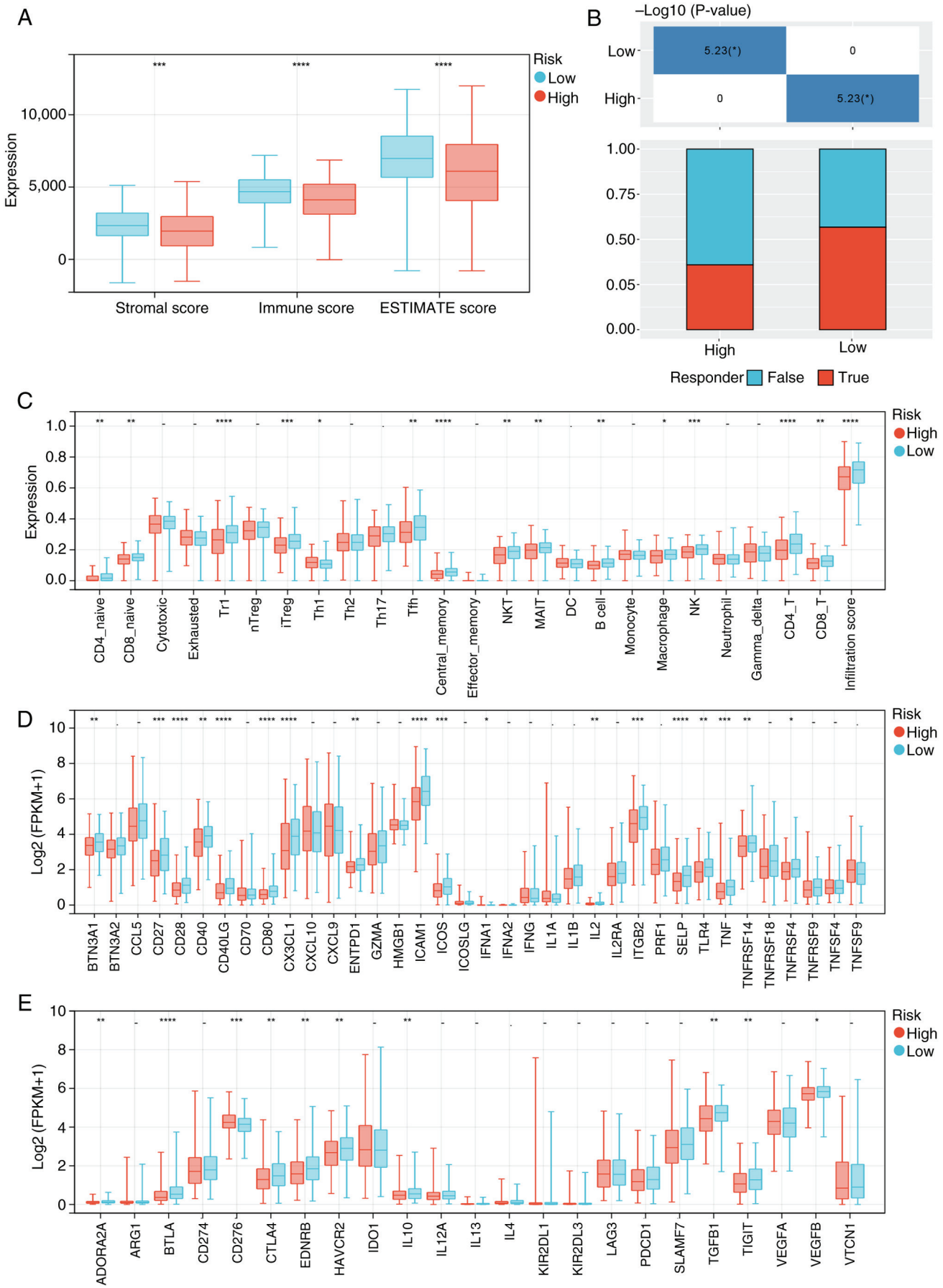

Figure 7. Immune infiltration and immune association analyses. Differences in (A) immune, stromal and ESTIMATE scores, (B) immune-checkpoint blockade therapy response prediction and (C) immune cells between the high- and low-risk groups. Differences in the expression of immune-checkpoint (D) immune stimulated and (E) immune inhibited genes between the high- and low-risk groups. *P<0.05; **P<0.01; ***P<0.001; ***P<0.0001. -, not significant; FPKM, fragments per kilobase of transcript per million mapped reads.

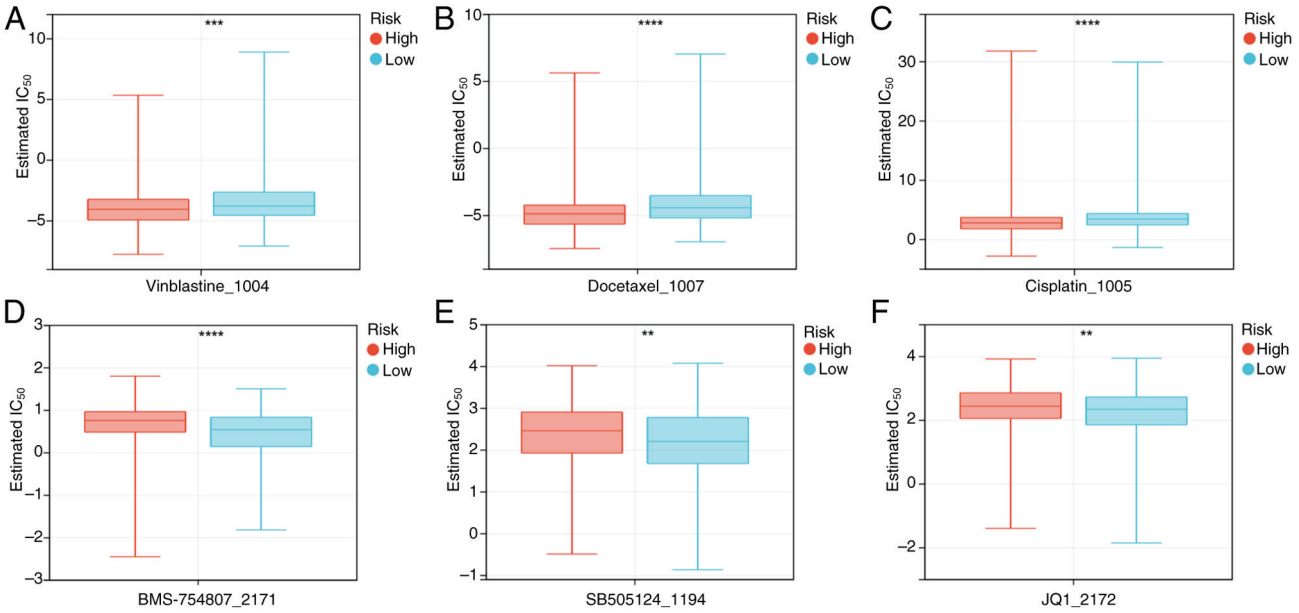

Figure 8. Differences in drug sensitivity between high- and low-risk groups. IC_{50} values for (A) vinblastine, (B) docetaxel and (C) cisplatin, which were more sensitive in the high-risk group. IC_{50} values for (D) BMS-754804, (E) SB05124 and (F) JQ1, which were more sensitive in the low-risk group. $^{**}P<0.01$; $^{***}P<0.001$; $^{****}P<0.0001$.

a crucial role in the tumor immune microenvironment (46). Therefore, increased infiltration of these cells may explain why the low-risk group exhibited improved prognosis compared with the high-risk group.

At present, research on immune checkpoint inhibitors is a hot topic. The current study assessed the expression of immune checkpoint suppressor genes in both the high- and low-risk groups. The results revealed high expression of immune checkpoint inhibitors, including CTLA4, T cell immunoreceptor with Ig and ITIM domains (TIGIT), HAVCR2 and B and T lymphocyte associated protein (BTLA) in the low-risk group. CTLA4 is a suppressor molecule located on the surface of T cells that can promote tumor tolerance and T-cell exhaustion when abnormally expressed (47). TIGIT is an immune checkpoint gene expressed on several types of T and NK cells. Its binding to CD155 on immune-suppressive cells or tumor cell surfaces inhibits immune cell function (48). HAVCR2, as a negatively regulated immune checkpoint, not only regulates the exhaustion of T and NK cells, but also regulates the intrinsic immune escape of tumors mediated by macrophages and dendritic cells (49). BTLA is a suppressor expressed on the surface of immune cells such as T and B cells. Upon binding to herpesvirus entry mediator, it sends inhibitory signals to T cells, leading to a decrease in T cell proliferation and activation (50). These findings indicate that there are more immunotherapeutic targets within the low-risk group with higher potential benefits from immunotherapy compared with the high-risk group, aligning with the predicted response rate for immunotherapy.

Notably, chemotherapy is a crucial component of LUAD treatment. Half-maximal inhibitory concentration analysis was performed to screen potential compounds and the findings revealed that the high-risk group exhibited greater sensitivity to vincristine, docetaxel and cisplatin, whilst the low-risk group showed increased sensitivity to BMS_754807, SB505124_1194 and JQ1_2172. Clinically, vincristine, docetaxel and cisplatin are commonly utilized chemotherapeutic agents for LUAD treatment, which are often administered in combination to enhance patient prognosis (51). BMS-754807 is a potent inhibitor of the insulin-like growth factor 1 receptor/insulin receptor family of kinases that synergistically interacts with platinum-based chemotherapeutics to induce apoptosis in lung cancer cells (52). Furthermore, dasatinib combined with BMS-754807 could inhibit lung cancer cell proliferation by inducing autophagy and arresting the cell cycle at G1 phase (53). SB505124_1194 is a selective TGF-β1 receptor inhibitor that notably impedes TGF-β1-mediated EMT in lung cancer cells, thereby reducing recurrence and metastasis (54,55). In the present study, higher expression of TGF-β1 in the low-risk group was associated with drug prediction. JQ1_2172 is a small molecule inhibitor targeting the BET protein that binds reversibly to its bromodomain, thus disrupting its interaction with acetylated lysines on histones or transcription factors. This inhibition leads to the suppression of oncogene expression, ultimately resulting in cancer cell proliferation arrest (56). Additionally, JQ1_2172 inhibits the upregulation of programmed death-ligand 1 during concurrent radiotherapy for lung cancer, thus exerting antitumor immune escape effects (57). Despite their effective eradication of tumor cells, anti-neoplastic drugs exert certain effects on both patients and hospital workers exposed to them, including increased DNA damage, elevated oxidative stress parameters and impairment on complete blood counts (58). Therefore, the implementation of personalized treatment strategies based on risk score could facilitate the selection of appropriate drug treatment plans, thereby enhancing treatment efficacy and minimizing the adverse effects of anti-neoplastic drugs on patients and healthcare workers.

Although a robust prognostic model based on KNHMUGs was constructed in the present study using public data, it is

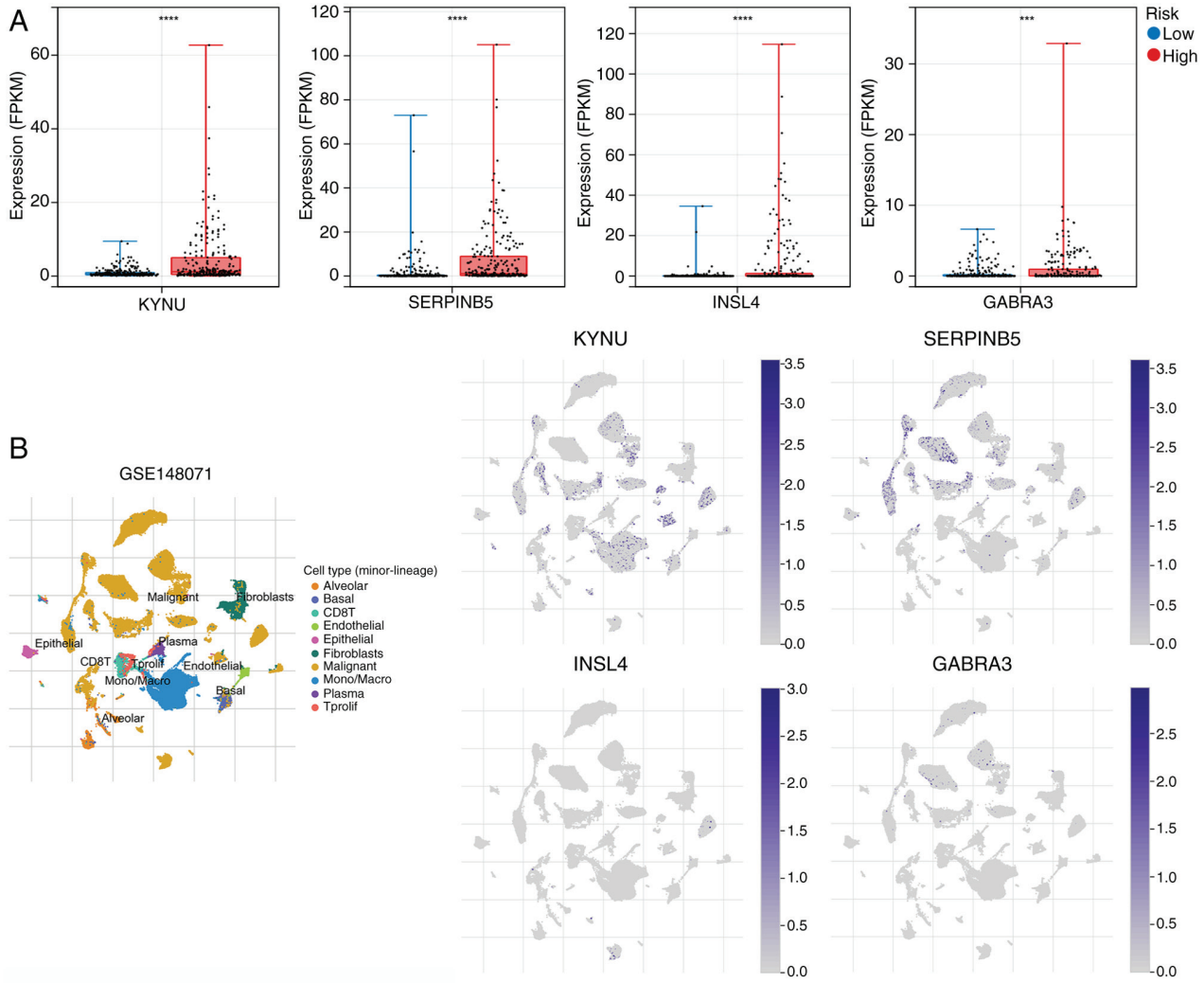

Figure 9. Expression of hub genes in different risk groups and their localization in lung adenocarcinoma. Expression of KYNU, SERPINB5, INSL4 and GABRA3 in (A) high- and low-risk groups, and (B) different cell types in the GSE148071 dataset. ***P<0.001, ****P<0.0001. KYNU, kynureninase; SERPINB5, serpin family B member 5; INSL4, insulin like 4; GABRA3, γ-aminobutyric acid type A receptor subunit α3; FPKM, fragments per kilobase of transcript per million mapped reads.

limited by several factors. Firstly, the current study solely relied on public databases and further clinical validation is therefore required to confirm the model efficacy in prognostic prediction and assessment of immunotherapy and chemotherapy sensitivity. Secondly, whilst the hub genes screened in the present study have been investigated in a small number of LUAD cases, their mechanisms remain unclear and require further exploration. Subsequent studies should be conducted to address the aforementioned questions.

In summary, KEAP1, NRF2 and HO-1 expression is closely associated with clinicopathological features and prognosis in LUAD. The prognostic model constructed based on KNHMUGs may serve as an independent prognostic factor for predicting the prognosis of patients with LUAD. It integrates important clinical parameters and risk scores of prognoses, demonstrating reliability and effectiveness. Furthermore, the association between risk score and tumor immune microenvironment, immunotherapy and chemotherapy response may offer a potentially powerful new tool for clinical decision-making, patient prognosis determination and personalized treatment.

Acknowledgements

Not applicable.

Funding

The present research was supported by the scientific research projects of the Top Talent Support Program for Young and Middle-Aged People of Wuxi Health Committee (grant no. HB2023116) and the Innovation Cultivation Fund of Xishan People's Hospital (grant no. 202103).

Availability of data and materials

The data generated in the present study may be requested from the corresponding author.

Authors' contributions

ZX designed the research and drafted the manuscript. CC and QS utilized software code to perform an in-depth analysis

and visualization of the data and reviewed the present paper. WZ and YZ analyzed the paraffin sections. LY designed the mathematical methods, collected and analyzed the data. LC performed the immunohistochemistry. WZ and ZX confirm the authenticity of all the raw data. All authors read and approved the final manuscript.

Ethics approval and consent to participate

The present study complied with the Declaration of Helsinki and was approved by the Xishan People's Hospital Ethics Committee (approval no. xs2024ky037). The samples used in the present study were sourced from Xishan People's Hospital in Wuxi City, collected from patients with LUAD undergoing surgery between January 2020 and June 2023. Written informed consent forms were signed by all patients.

Patient consent for publication

Not applicable.

Competing interests

The authors declare that they have no competing interests.

References

1. Sung H, Ferlay J, Siegel RL, Laversanne M, Soerjomataram I, Jemal A and Bray F: Global cancer statistics 2020: GLOBOCAN estimates of incidence and mortality worldwide for 36 cancers in 185 countries. CA Cancer J Clin 71: 209-249, 2021.
2. Denisenko TV, Budkevich IN and Zhivotovsky B: Cell death-based treatment of lung adenocarcinoma. Cell Death Dis 9: 117, 2018.
3. Reck M and Rabe KF: Precision diagnosis and treatment for advanced non-small-cell lung cancer. N Engl J Med 377: 849-861, 2017.
4. Li Y, Yan B and He S: Advances and challenges in the treatment of lung cancer. Biomed Pharmacother 169: 115891, 2023.
5. Obradovic J, Todosijevic J and Jurisic V: Application of the conventional and novel methods in testing EGFR variants for NSCLC patients in the last 10 years through different regions: A systematic review. Mol Biol Rep 48: 3593-3604, 2021.
6. Jurisic V, Vukovic V, Obradovic J, Gulyaeva LF, Kushlinskii NE and Djordjevic N: EGFR polymorphism and survival of NSCLC patients treated with TKIs: A systematic review and meta-analysis. J Oncol 2020: 1973241, 2020.
7. Obradovic J, Todosijevic J and Jurisic V: Side effects of tyrosine kinase inhibitors therapy in patients with non-small cell lung cancer and associations with EGFR polymorphisms: A systematic review and meta-analysis. Oncol Lett 25: 62, 2023.
8. Xu K, Ma J, Hall SRR, Pengs RW, Yang H and Yao F: Battles against aberrant KEAP1-NRF2 signaling in lung cancer: Intertwined metabolic and immune networks. Theranostics 13: 704-723, 2023.
9. Ghareghomi S, Moosavi-Movahedi F, Saso L, Habibi-Rezaei M, Khatibi A, Hong J and Moosavi-Movahedi AA: Modulation of Nrf2/HO-1 by natural compounds in lung cancer. Antioxidants (Basel) 12: 735, 2023.
10. Imielinski M, Berger AH, Hammerman PS, Hernandez B, Pugh TJ, Hodis E, Cho J, Suh J, Capelletti M, Sivachenko A, *et al*: Mapping the hallmarks of lung adenocarcinoma with massively parallel sequencing. Cell 150: 1107-1120, 2012.
11. Romero R, Sanchez-Rivera FJ, Westcott PMK, Mercer KL, Bhutkar A, Muir A, Robles TJ, Rodríguez SL, Liao LZ, Ng SR, *et al*: Keap1 mutation renders lung adenocarcinomas dependent on Slc33a1. Nat Cancer 1: 589-602, 2020.
12. Romero R, Sayin VI, Davidson SM, Bauer MR, Singh SX, LeBoeuf SE, Karakousi TR, Ellis DC, Bhutkar A, Sánchez-Rivera FJ, *et al*: Keap1 loss promotes Kras-driven lung cancer and results in dependence on glutaminolysis. Nat Med 23: 1362-1368, 2017.
13. Zavitsanou AM, Pillai R, Hao Y, Wu WL, Bartnicki E, Karakousi T, Rajalingam S, Herrera A, Karatza A, Rashidfarrokhi A, *et al*: KEAP1 mutation in lung adenocarcinoma promotes immune evasion and immunotherapy resistance. Cell Rep 42: 113295, 2023.
14. Ghareghomi S, Habibi-Rezaei M, Arese M, Saso L and Moosavi-Movahedi AA: Nrf2 modulation in breast cancer. Biomedicines 10: 2668, 2022.
15. Menegon S, Columbano A and Giordano S: The dual roles of NRF2 in cancer. Trends Mol Med 22: 578-593, 2016.
16. Kerins MJ and Ooi A: A catalogue of somatic NRF2 gain-of-function mutations in cancer. Sci Rep 8: 12846, 2018.
17. Li C, Liang G, Yan K and Wang Y: NRF2 mutation enhances the immune escape of hepatocellular carcinoma by reducing STING activation. Biochem Biophys Res Commun 698: 149536, 2024.
18. Tang H, Liu S, Yan X, Jin Y, He X, Huang H, Liu L, Hu W and Wu A: Inhibition of LNC EBLN3P enhances radiation-induced mitochondrial damage in lung cancer cells by targeting the Keap1/Nrf2/HO-1 axis. Biology (Basel) 12: 1208, 2023.
19. Spampinato M, Sferrazzo G, Pittala V, Di Rosa M, Vanella L, Salerno L, Sorrenti V, Carota G, Parrinello N, Raffaele M, *et al*: Non-competitive heme oxygenase-1 activity inhibitor reduces non-small cell lung cancer glutathione content and regulates cell proliferation. Mol Biol Rep 47: 1949-1964, 2020.
20. Director's Challenge Consortium for the Molecular Classification of Lung Adenocarcinoma, Shedden K, Taylor JM, Enkemann SA, Tsao MS, Yeatman TJ, Gerald WL, Eschrich S, Jurisica I, Giordano TJ, *et al*: Gene expression-based survival prediction in lung adenocarcinoma: A multi-site, blinded validation study. Nat Med 14: 822-827, 2008.
21. Lanczky A and Gyorffy B: Web-based survival analysis tool tailored for medical research (KMplot): Development and implementation. J Med Internet Res 23: e27633, 2021.
22. Ritchie ME, Phipson B, Wu D, Hu Y, Law CW, Shi W and Smyth GK: limma powers differential expression analyses for RNA-sequencing and microarray studies. Nucleic Acids Res 43: e47, 2015.
23. Liu Z, Liu L, Weng S, Guo C, Dang Q, Xu H, Wang L, Lu T, Zhang Y, Sun Z and Han X: Machine learning-based integration develops an immune-derived lncRNA signature for improving outcomes in colorectal cancer. Nat Commun 13: 816, 2022.
24. Miao YR, Zhang Q, Lei Q, Luo M, Xie GY, Wang H and Guo AY: ImmuCellAI: A unique method for comprehensive T-cell subsets abundance prediction and its application in cancer immunotherapy. Adv Sci (Weinh) 7: 1902880, 2020.
25. Maeser D, Gruener RF and Huang RS: oncoPredict: An R package for predicting in vivo or cancer patient drug response and biomarkers from cell line screening data. Brief Bioinform 22: bbab260, 2021.
26. Detterbeck FC, Woodard GA, Bader AS, Dacic S, Grant MJ, Park HS and Tanoue LT: The proposed ninth edition TNM classification of lung cancer. Chest 166: 882-895, 2024.
27. Lou JS, Zhao LP, Huang ZH, Chen XY, Xu JT, Tai WC, Tsim KWK, Chen YT and Xie T: Ginkgetin derived from Ginkgo biloba leaves enhances the therapeutic effect of cisplatin via ferroptosis-mediated disruption of the Nrf2/HO-1 axis in EGFR wild-type non-small-cell lung cancer. Phytomedicine 80: 153370, 2021.
28. Bi G, Liang J, Zhao M, Zhang H, Jin X, Lu T, Zheng Y, Bian Y, Chen Z, Huang Y, *et al*: miR-6077 promotes cisplatin/pemetrexed resistance in lung adenocarcinoma via CDKN1A/cell cycle arrest and KEAP1/ferroptosis pathways. Mol Ther Nucleic Acids 28: 366-386, 2022.
29. Mei L, Long J, Wu S, Mei M, Mei D and Qiu H: APOC1 reduced anti-PD-1 immunotherapy of nonsmall cell lung cancer via the transformation of M2 into M1 macrophages by ferroptosis by NRF2/HO-1. Anticancer Drugs 35: 333-343, 2024.
30. Wei XW, Lu C, Zhang YC, Fan X, Xu CR, Chen ZH, Wang F, Yang XR, Deng JY, Yang M, *et al*: Redox(high) phenotype mediated by KEAP1/STK11/SMARCA4/NRF2 mutations diminishes tissue-resident memory CD8+ T cells and attenuates the efficacy of immunotherapy in lung adenocarcinoma. Oncoimmunology 13: 2340154, 2024.
31. Fahrmann JF, Tanaka I, Irajizad E, Mao X, Dennison JB, Murage E, Casabar J, Mayo J, Peng Q, Celiktas M, *et al*: Mutational activation of the NRF2 pathway upregulates kynureninase resulting in tumor immunosuppression and poor outcome in lung adenocarcinoma. Cancers (Basel) 14: 2543, 2022.

32. Phillips RS: Structure and mechanism of kynureninase. Arch Biochem Biophys 544: 69-74, 2014.
33. Karayama M, Masuda J, Mori K, Yasui H, Hozumi H, Suzuki Y, Furuhashi K, Fujisawa T, Enomoto N, Nakamura Y, *et al*: Comprehensive assessment of multiple tryptophan metabolites as potential biomarkers for immune checkpoint inhibitors in patients with non-small cell lung cancer. Clin Transl Oncol 23: 418-423, 2021.
34. Leon-Letelier RA, Sater AH, Chen Y, Park S, Wu R, Irajizad E, Dennison JB, Katayama H, Vykoukal JV, Hanash S, *et al*: Kynureninase upregulation is a prominent feature of NFR2-activated cancers and is associated with tumor immunosuppression and poor prognosis. Cancers (Basel) 15: 834, 2023.
35. Liu BX, Xie Y, Zhang J, Zeng S, Li J, Tao Q, Yang J, Chen Y and Zeng C: SERPINB5 promotes colorectal cancer invasion and migration by promoting EMT and angiogenesis via the TNF-α/NF-κB pathway. Int Immunopharmacol 131: 111759, 2024.
36. Rathod M, Franz H, Beyersdorfer V, Wanuske MT, Leal-Fischer K, Hanns P, Stüdle C, Zimmermann A, Buczak K, Schinner C and Spindler V: DPM1 modulates desmosomal adhesion and epidermal differentiation through SERPINB5. J Cell Biol 223: e202305006, 2024.
37. He X, Ma Y, Huang Z, Wang G, Wang W, Zhang R, Guo G, Zhang X, Wen Y and Zhang L: SERPINB5 is a prognostic biomarker and promotes proliferation, metastasis and epithelial-mesenchymal transition (EMT) in lung adenocarcinoma. Thorac Cancer 14: 2275-2287, 2023.
38. Scopetti D, Piobbico D, Brunacci C, Pieroni S, Bellezza G, Castelli M, Ludovini V, Tofanetti FR, Cagini L, Sidoni A, *et al*: INSL4 as prognostic marker for proliferation and invasiveness in non-small-cell lung cancer. J Cancer 12: 3781-3795, 2021.
39. Yang R, Li SW, Chen Z, Zhou X, Ni W, Fu DA, Lu J, Kaye FJ and Wu L: Role of INSL4 signaling in sustaining the growth and viability of LKB1-inactivated lung cancer. J Natl Cancer Inst 111: 664-674, 2019.
40. Bhattacharya D, Gawali VS, Kallay L, Toukam DK, Koehler A, Stambrook P, Krummel DP and Sengupta S: Therapeutically leveraging GABA(A) receptors in cancer. Exp Biol Med (Maywood) 246: 2128-2135, 2021.
41. Liu L, Yang C, Shen J, Huang L, Lin W, Tang H, Liang W, Shao W, Zhang H and He J: GABRA3 promotes lymphatic metastasis in lung adenocarcinoma by mediating upregulation of matrix metalloproteinases. Oncotarget 7: 32341-32350, 2016.
42. Hanahan D and Coussens LM: Accessories to the crime: Functions of cells recruited to the tumor microenvironment. Cancer Cell 21: 309-322, 2012.
43. Binnewies M, Roberts EW, Kersten K, Chan V, Fearon DF, Merad M, Coussens LM, Gabrilovich DI, Ostrand-Rosenberg S, Hedrick CC, *et al*: Understanding the tumor immune microenvironment (TIME) for effective therapy. Nat Med 24: 541-550, 2018.
44. Genova C, Dellepiane C, Carrega P, Sommariva S, Ferlazzo G, Pronzato P, Gangemi R, Filaci G, Coco S and Croce M: Therapeutic implications of tumor microenvironment in lung cancer: Focus on immune checkpoint blockade. Front Immunol 12: 799455, 2021.
45. Song P, Li W, Guo L, Ying J, Gao S and He J: Identification and validation of a novel signature based on NK cell marker genes to predict prognosis and immunotherapy response in lung adenocarcinoma by integrated analysis of single-cell and bulk RNA-sequencing. Front Immunol 13: 850745, 2022.
46. Terabe M and Berzofsky JA: Tissue-specific roles of NKT cells in tumor immunity. Front Immunol 9: 1838, 2018.
47. Rad SH, Monkman J, Warkiani ME, Ladwa R, O'Byrne K, Rezaei N and Kulasinghe A: Understanding the tumor microenvironment for effective immunotherapy. Med Res Rev 41: 1474-1498, 2021.
48. Ge Z, Peppelenbosch MP, Sprengers D and Kwekkeboom J: TIGIT, the next step towards successful combination immune checkpoint therapy in cancer. Front Immunol 12: 699895, 2021.
49. Acharya N, Sabatos-Peyton C and Anderson AC: Tim-3 finds its place in the cancer immunotherapy landscape. J Immunother Cancer 8: e000911, 2020.
50. Wojciechowicz K, Spodzieja M and Wardowska A: The BTLA-HVEM complex-The future of cancer immunotherapy. Eur J Med Chem 268: 116231, 2024.
51. Gebbia V, Lorusso V, Galetta D, Caruso MM, Palomba G, Riccardi F, Borsellino N, Carrozza F, Leo S, Ferraù F, *et al*: First-line cisplatin with docetaxel or vinorelbine in patients with advanced non-small-cell lung cancer: A quality of life directed phase II randomized trial of Gruppo Oncologico Italia Meridionale. Lung Cancer 69: 218-224, 2010.
52. Fuentes-Baile M, Ventero MP, Encinar JA, García-Morales P, Poveda-Deltell M, Pérez-Valenciano E, Barberá VM, Gallego-Plazas J, Rodríguez-Lescure Á, Martín-Nieto J and Saceda M: Differential effects of IGF-1r small molecule tyrosine kinase inhibitors BMS-754807 and OSI-906 on human cancer cell lines. Cancers (Basel) 12: 3717, 2020.
53. Zhang C, Zhao X, Wang Z, Gong T, Zhao H, Zhang D, Niu Y, Li X, Zhao X, Li G, *et al*: Dasatinib in combination with BMS-754807 induce synergistic cytotoxicity in lung cancer cells through inhibiting lung cancer cell growth, and inducing autophagy as well as cell cycle arrest at the G1 phase. Invest New Drugs 41: 438-452, 2023.
54. DaCosta Byfield S, Major C, Laping NJ and Roberts AB: SB-505124 is a selective inhibitor of transforming growth factor-beta type I receptors ALK4, ALK5, and ALK7. Mol Pharmacol 65: 744-752, 2004.
55. Wu TH, Chou YW, Chiu PH, Tang MJ, Hu CW and Yeh ML: Validation of the effects of TGF-β1 on tumor recurrence and prognosis through tumor retrieval and cell mechanical properties. Cancer Cell Int 14: 20, 2014.
56. Stathis A and Bertoni F: BET proteins as targets for anticancer treatment. Cancer Discov 8: 24-36, 2018.
57. Wang J, Xu Y, Rao X, Zhang R, Tang J, Zhang D, Jie X, Zhu K, Wang X, Xu Y, *et al*: BRD4-IRF1 axis regulates chemoradiotherapy-induced PD-L1 expression and immune evasion in non-small cell lung cancer. Clin Transl Med 12: e718, 2022.
58. Mrdjanovic J, Solajic S, Srdenovic-Conic B, Bogdanović V, Dea KJ, Kladar N and Jurišić V: The oxidative stress parameters as useful tools in evaluating the DNA damage and changes in the complete blood count in hospital workers exposed to low doses of antineoplastic drugs and ionizing radiation. Int J Environ Res Public Health 18: 8445, 2021.